Yazawa's Diagram

G M Willis[1] and J M Toguri[2]

ABSTRACT

Phase diagrams using chemical potentials as coordinates, such as those introduced by Yazawa (1974), have been developed for multiple phase systems up to quaternary.

INTRODUCTION

Yazawa's diagram

This work grew from conversation with the late Professor J M Toguri on the derivation of Yazawa's well-known diagram for copper smelting and converting (Figure 1, Yazawa, 1974). It was not obvious how log P_{O_2} versus log P_{S_2} diagrams for iron and for copper were combined in the four-component system. SiO_2 is not considered as a component here as the system is saturated with it. Ternary log-log diagrams are discussed later.

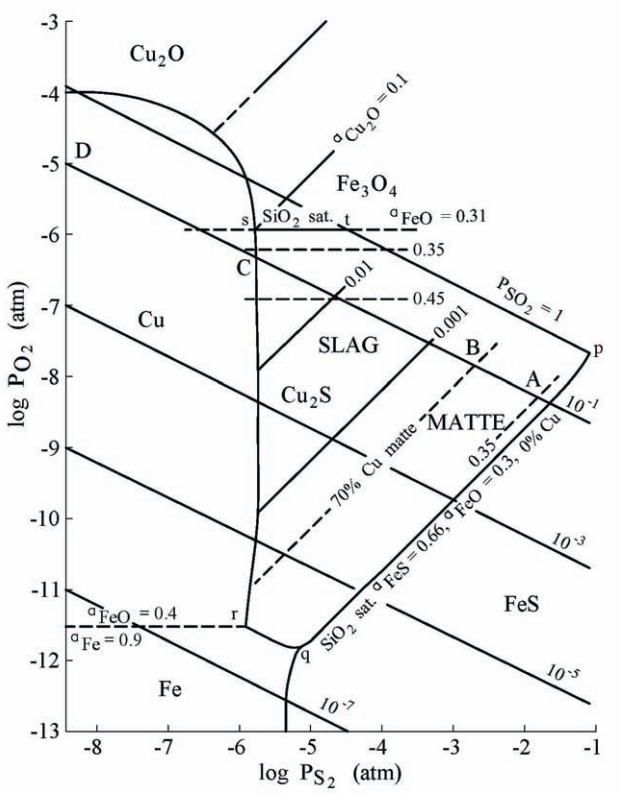

FIG 1 - The Yazawa diagram for copper smelting and converting. (Yazawa, 1974).

The origin of lines of constant matte grade was not clear, nor was a method for obtaining similar diagrams for other non-ferrous metals such as nickel, lead and tin.

In due course it was realised that Yazawa's log P_{O_2} versus log P_{S_2} diagram is a projection of a three-dimensional figure on to this plane. A third axis, normal to this plane is matte grade.

The phase rule

The Gibbs-Duhem equation:

$$SdT - VdP + n_1 d\mu_1 + n_2 d\mu_2 + \ldots. n_c d\mu_c = 0 \quad (1)$$

for a single phase of **C** components has **C**+2 variables of which **C**+1 can be chosen, ie there are **C**+1 degrees of freedom, where:

S = entropy

T = absolute temperature

V = volume

P = pressure

n_i = the number of modes of the i^{th} component

μ_i = the chemical potential of the i^{th} component

$$\mu_i = \left(\frac{\partial G}{\partial n_i}\right)_{T,P,n_1,n_2,\ldots n_c \neq n_i} \quad (2)$$

A second phase will have a similar Gibbs-Duhem equation, and in equilibrium with the first phase, the same values of T, P and chemical potentials (μ_i). There will be a similar restriction on the degrees of freedom because of its particular Gibbs-Duhem equation, so the degrees of freedom are reduced to C. Other equilibrium phases similarly reduce the number of degrees of freedom by one for each phase. This leads to the phase rule in the form:

$$\mathbf{F = C + 2 - P} \quad (3)$$

where:

P is the number of phases

It may be noted that *composition* of the phases is not used here.

Since F cannot be less than zero, the maximum number of co-existing equilibrium phases in any system is C + 2. The triple point in a one-compound system is a familiar example. That for arsenic (Baker, 1974) is shown in Figure 2.

TYPES OF PHASE DIAGRAMS

The literature shows many different types of equilibrium diagrams.

Pelton and Schmalzried (1973) recognised three fundamental types of phase diagrams using two sets of variables. The first comprise thermodynamic potentials and at temperature T, pressure P and chemical potentials:

$$\mu_i = \left(\frac{\partial G}{\partial n_i}\right)_{T,P,n_1,n_2,\ldots n_c \neq n_i} \quad (2)$$

Their composition variable is the ratio of conjugate extensive variables. For most purposes, any monotonic function of the ratio can be used, eg instead of n_A/n_B one can use the mole-fraction $n_A/(n_A + n_B)$. The three types of diagrams are:

1. MAusIMM, PO Box 77, Blairgowrie Vic 3942.

2. Formerly: Department of Metallurgy and Materials Science, University of Toronto, 27 King's College Circle, Toronto ON M5S 1A1, Canada.

1. using two thermodynamic potentials, eg P and T;
2. one thermodynamic potential and one ratio (eg T, N_A or equivalent); and
3. both functions are ratios of extensive variable, eg $n_A/(n_A + n_B)$ and $n_C/(n_A + n_B)$.

Pelton and Schmalzried make the important observation that the topography of all these diagrams is similar:

1. P versus T, eg H_2O or As;
2. RTln P_{O_2} versus T for a metal-oxygen system, eg FeO, PbO, CuO; and
3. in the system ABC, the composition can be given as mol fraction or as: $X_A = n_A/(n_A + n_B)$ and $X_C = n_C/(n_A + n_B)$ or n_B/n_C and n_A/n_C.

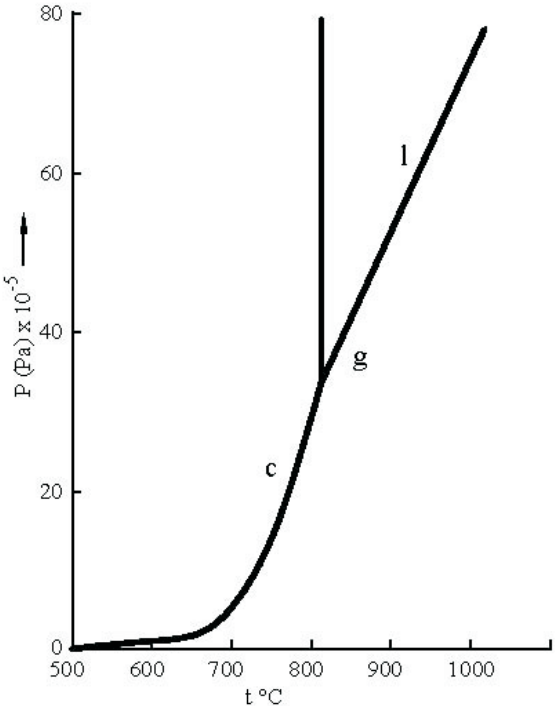

FIG 2 - Pressure-temperature curves for arsenic (Baker, 1974).

TWO-COMPONENT SYSTEMS

Ellingham diagrams (Ellingham, 1944) are well-known examples of phase diagrams using two potentials – the chemical potential of O_2, RTln P_{O_2} and the temperature. They are plots of the standard free energy of formation ΔG° per mole of O_2, against temperature. For the reaction $M + O_2 = MO_2$:

$$K = a_{MO_2} / a_M \cdot P_{O_2} \tag{4}$$

$$\Delta G^\circ = -RT \ln K \tag{5}$$

$$= RT \ln P_{O_2} \left(\frac{a_M}{a_{MO_2}} \right) \tag{6}$$

With both metal and oxide in their standard states their activities are one, and:

$$\Delta G^\circ \equiv RT \ln P_{O_2} \tag{7}$$

Since $\frac{\partial(\Delta G^\circ)}{\partial T} = -\Delta S^\circ$, and because the entropy of gaseous O_2 is much greater than that of the condensed metal or oxide phase, ΔS° is negative, so the lines have a positive slope. If there is a change in phase such as melting, there is an associated change in entropy, and hence change in slope. Figure 3 shows the Ellingham diagram for the lead-oxygen system. The changes in slope are readily seen.

The line separates metal and oxide phases, and so is a phase boundary. A third vertical line which is conventionally omitted occurs at a phase change (see Figure 3). This third line satisfies the requirement that three lines meet at an invariant point.

Figure 4 shows the effect of the large increase in entropy when zinc vapour becomes stable; there is a corresponding large increase in the slope of the ΔG versus T line.

In real systems the co-existing phases may not be in their standard states. Figure 5 based on Schmid's assessment of the copper-oxygen system (Schmid, 1983) where the composition, particularly of liquid phases, changes substantially with temperature. The conventional temperature-composition diagram can be recognised in a distorted form.

Similar diagrams for sulfide systems, where liquids are often present at smelting temperature, are shown for copper-sulfur (Sharma and Chang, 1980), iron-sulfur (Sharma and Chang, 1979)

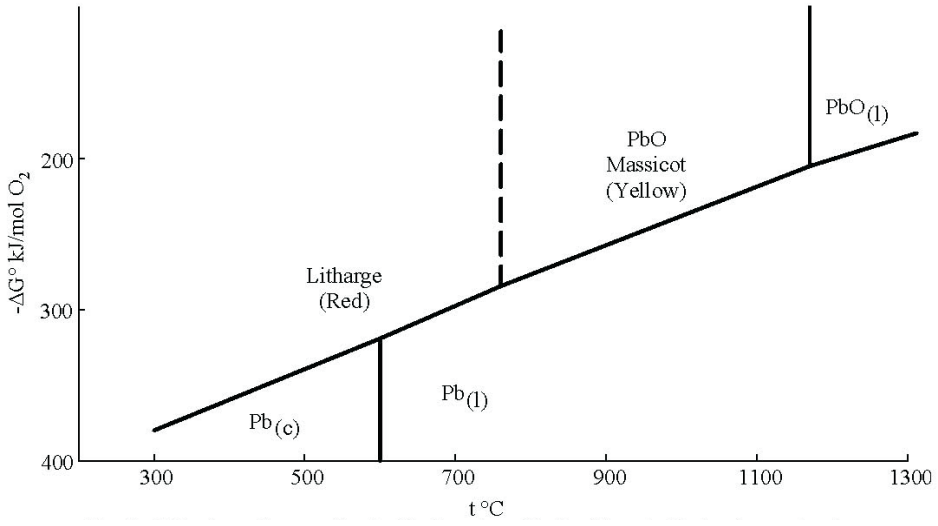

FIG 3 - Ellingham diagram for the Pb-O system. Vertical lines indicate changes in phase.

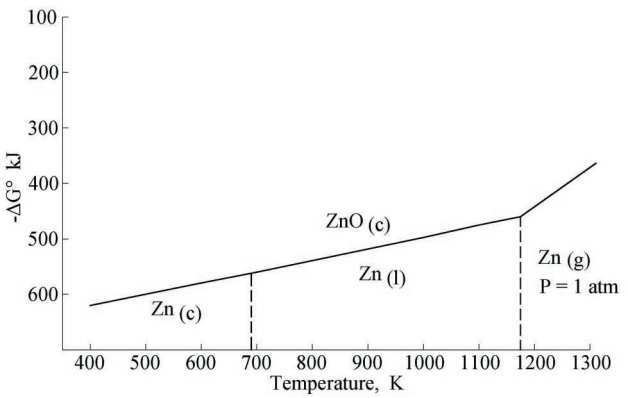

FIG 4 - The Zn-O system.

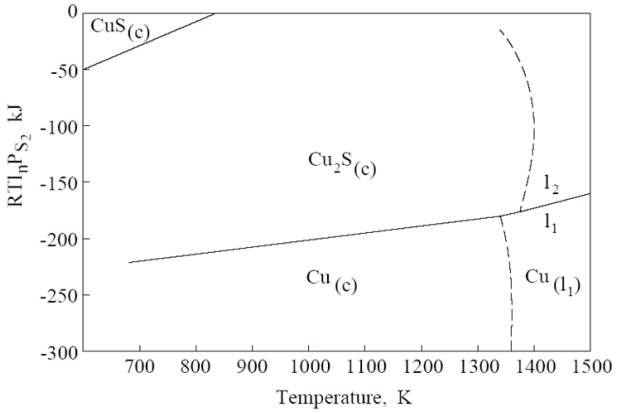

FIG 6 - The Cu-S system (Sharma and Chang, 1980).

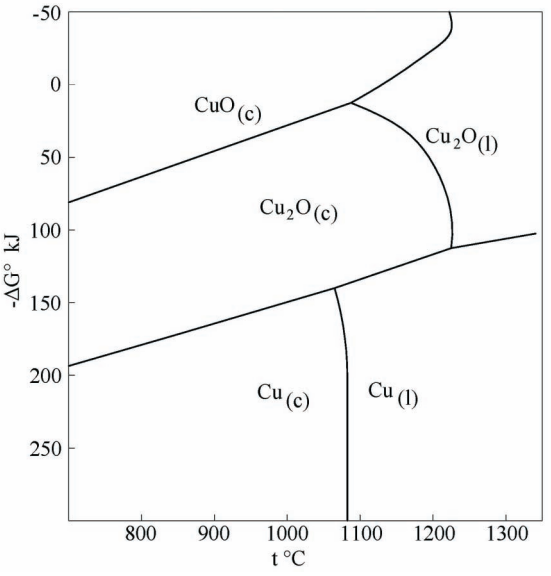

FIG 5 - The Cu-O system (based on Schmid, 1983).

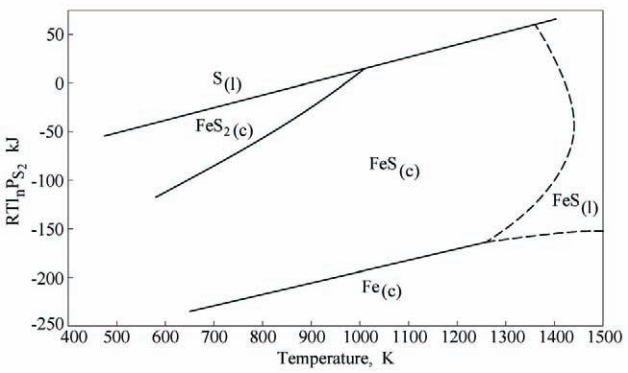

FIG 7 - The Fe-S system (Sharma and Chang, 1979).

and lead-sulfur (Lin, Sharma and Chang, 1986) in Figures 6, 7 and 8 respectively. The great disparity between the standard free energy line, and the actual phase boundary with lead is due to the extremely high solubility of sulfur in lead at temperatures around the melting point of galena.

It is commonly recognised that in Ellingham diagrams for sulfides, the lines for the common heavy metals are comparatively close together. This is also to be seen for the liquid sulfides, which cover similar ranges of sulfur potential at temperatures above their melting points – compare Figures 6, 7 and 8.

TERNARY SYSTEMS

Two types of diagrams are important for ternary systems. The first uses the chemical potentials of two components in an isothermal system and is exemplified by Kellogg's 'thermodynamic phase diagrams' for the lead-sulfur-oxygen system (Kellogg and Basu, 1960) where the stable phases are shown in a plot of log P_{SO_2} versus log P_{O_2}.

Diagrams of this type can be readily derived for metal-sulfur-oxygen systems. Starting with the pure metal, if P_{O_2} is increased eventually the oxide phase will become stable, as shown by a horizontal line in Figure 9, as P_{S_2} is of no effect, until it is high enough for the sulfide to be stable. This is shown by the vertical boundary *M*/*MS* in Figure 9.

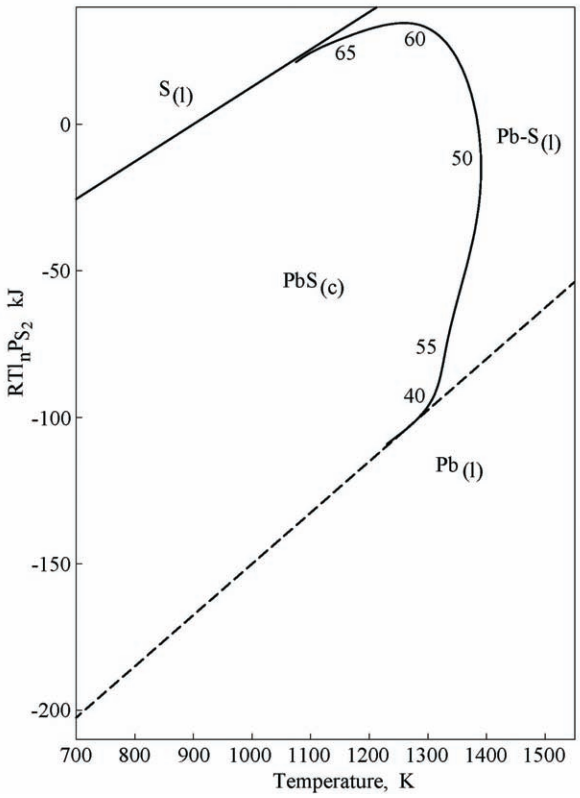

FIG 8 - The Pb-S system. (The broken line is that for ΔG°. Numbers are atomic per cent sulfur in melt.)

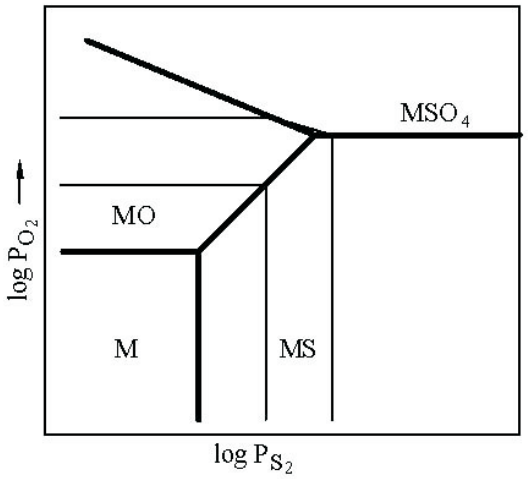

FIG 9 - Schematic diagram of the M-S-O system with log P_{O_2} and log P_{S_2} as variables. P and T both constant. Lighter lines are lines of constant metal activity.

The two lines meet at a triple point, where a new pair of stable phases – oxide and sulfide co-exist over a range of P_{O_2} and P_{S_2}. For MO and MS, we have:

$$MO + \tfrac{1}{2} S_{2(g)} = MS + \tfrac{1}{2} O_{2(g)} \quad (8)$$

$$K = a_{MS} / a_{MO} \cdot (P_{O_2} / P_{S_2})^{\frac{1}{2}} \quad (9)$$

and for the oxide and sulfide both in their standard states we have:

$$\log K = \frac{1}{2} \cdot (\log P_{O_2} - \log P_{S_2}) \quad (10)$$

which gives the oxide-sulfide boundary as a line of unit slope. Similar equations written always in terms of O_2 and S_2 give boundaries for other phases, such as the sulfate shown schematically in Figure 9.

Ingraham gives P_{SO_3} versus P_{O_2} diagrams for Co-S-O (1964), Ni-S-O (1966) Cu-S-O (1965) and Mn-S-O (1966) while Ingraham and Kellogg (1963) give Zn-S-O.

Similar diagrams can be drawn for systems with, for example, arsenic as in the Fe-As-O system in Figure 10, derived from the results of Chakraborti and Lynch (1983). Skeaff, Mainwaring and Speelman (1985) give the Ni-As-O system in terms of log $P_{As_4O_6}$ and log P_{O_2}.

Matte-speiss equilibria can be given by log a_{As} versus log P_{S_2} diagrams as in Figure 11 for the Cu-As-S system calculated from the measurements of Hino and Toguri (personal communication).

Ternaries may also be represented by isothermal diagrams of chemical potential versus composition. Pelton and Schmalzried (1973) describe this and give examples. They can be derived by a method used by Korzhinskii (1959). In a ternary ABC, Figure 12, if a line is drawn from the C corner of the equilateral triangle to the base AB, the ratio of the number of moles n_A/n_B is constant along this line. This means, as the composition moves towards C along this line, the chemical potential of C increases because of the relation for a stable phase:

$$\left(\frac{\partial \mu_C}{\partial n_C}\right)_{T,P,n_A,n_B} \geq 0 \quad (11)$$

μ_c can then be plotted against n_A/n_B or more conventionally, $n_B/(n_A + n_B) = X_B$.

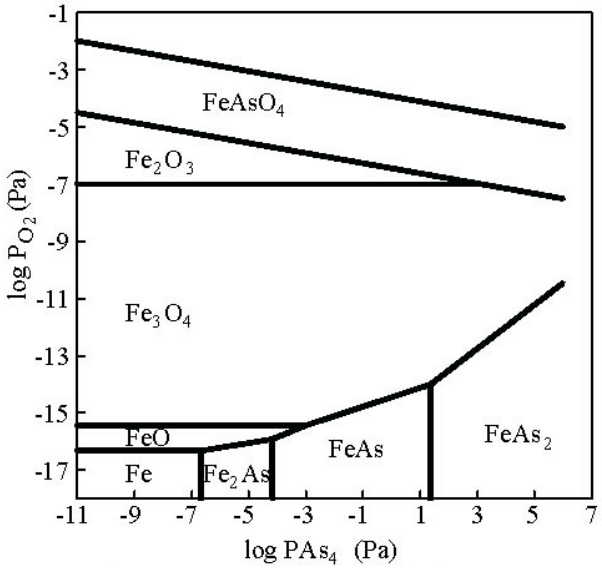

FIG 10 - Log P_{O_2} versus log P_{S_2} for the Fe-As-O system at 973°K (derived from results of Chakraborti and Lynch, 1983).

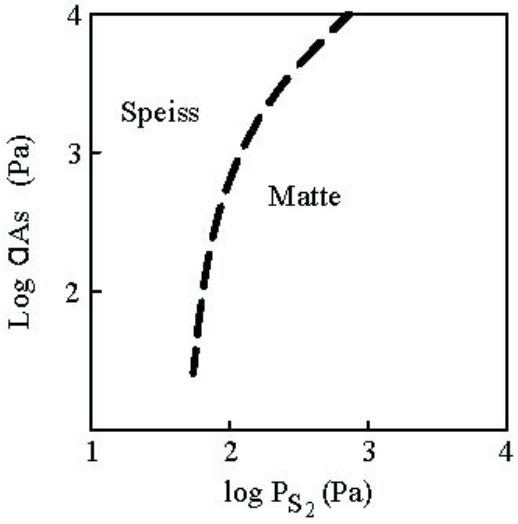

FIG 11 - The boundaries between matte and speiss for the Cu-As-S system. (Calculated from the measurements of Hino and Toguri, personal communication.)

An alternative derivation is given by Schmalzried and Pelton (1973). They call the quality X_B the mole ratio ξ, but there appears to be no fixed name for this. It can also be regarded as the C-face composition coordinate of a Jänecke diagram which has $n_C/(n_B + n_B)$ and $n_B/(n_A + n_B)$ as coordinates. Diagrams with μ_C versus X_B have tie-lines as horizontal lines, since the equilibrium phases have the same μ_C. (The other μ's are not shown.) Tie lines are generally not shown.

Two common types of diagram can be recognised. If there are two co-existing phases with composition running from the A side to the B side without intermediate phases, diagrams such as that for the Co-Fe-O system (Figure 13) are shown (Aukrust and Muan, 1964). The loop for the alloy – (Fe, Co)O equilibrium is for practically ideal solutions, which is not the case for the spinel-(Fe, Co)O region. The Fe-Ni-S system, Figure 14, has an unusually narrow loop (Willis). The Fe-Cu-S diagram resembles a eutectic alloy system, because of the immiscibility between iron and copper (Bale and Toguri, 1976), Figure 15.

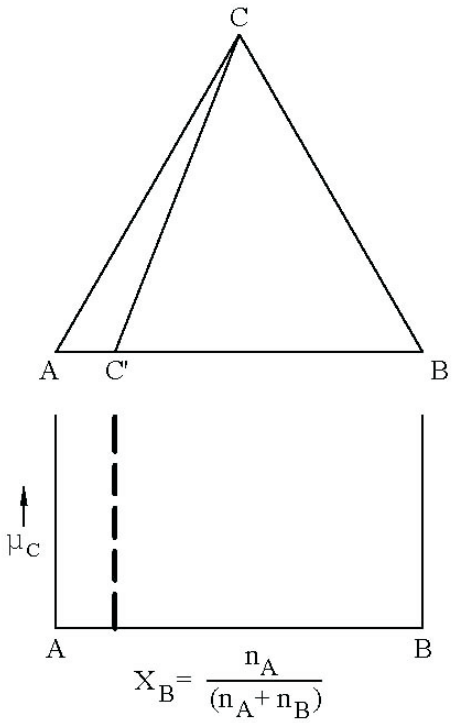

FIG 12 - Ternary ABC diagram.

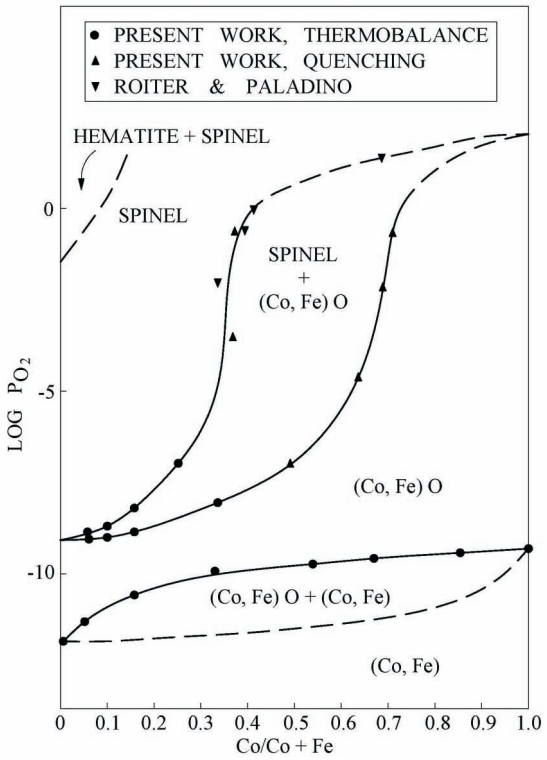

FIG 13 - Log P_{O_2} versus Co/Co+Fe for the Co-Fe-O system (from Aukrust and Muan, 1963).

Many diagrams are dominated by an intermediate phase, after a spinel solid solution in systems containing iron. The copper-iron-oxygen system, Figure 16 (Jacob, Fitzner and Alcock, 1977), is divided by the $CuFeO_2$ phase at high oxygen pressures and the spinel solid solution over a range of log P_{O_2}.

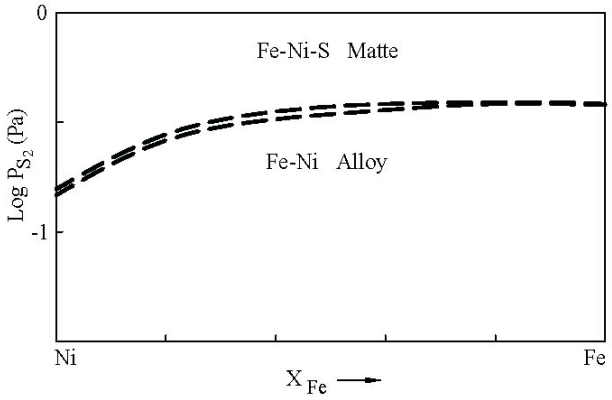

FIG 14 - The Fe-Ni-S system at 1200°C (Willis, unpublished).

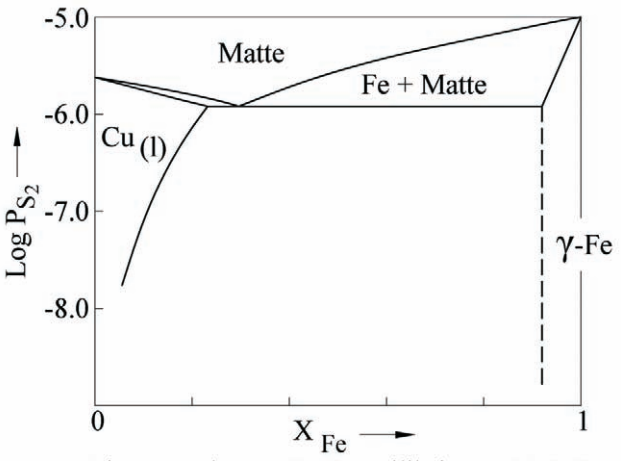

FIG 15 - The Fe-Cu-S equilibria at 1200°C (Bale and Toguri, 1976).

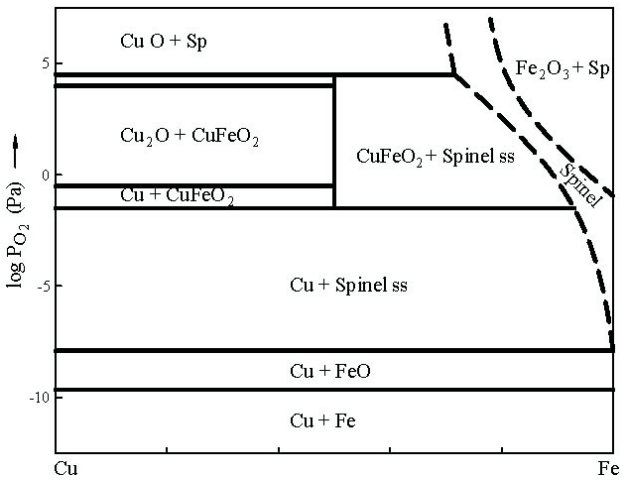

FIG 16 - Cu-Fe-O equilibria at 1100°C (Jacob, Fitzner and Alcock, 1977).

Miscibility gaps which close at high P_{S_2} are shown in the iron-lead-sulfur system (Figure 17) (Eric and Ozok, 1994). *Log* P_{S_2} versus X_{Cu} graphs for many ternary systems with Cu and S are given in the INCRA publication, *Phase Diagrams and Thermodynamic Properties of Ternary Copper-Sulphur-Metal Systems* (Chang, Neumann and Choudary, 1979).

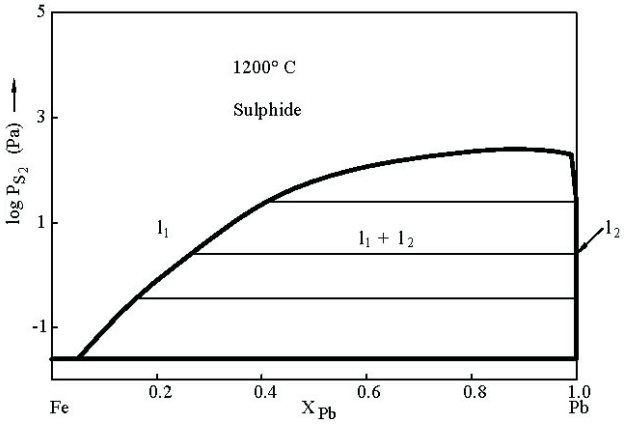

FIG 17 - The Fe-Pb-S system at 1200°C (Eric and Ozok, 1994).

FOUR COMPONENT SYSTEMS

The regular composition tetrahedron (Figure 18) can be converted to a three-dimensional diagram with two chemical potentials as axes.

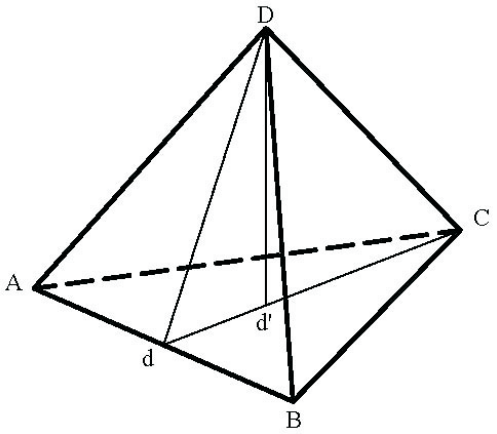

FIG 18 - Regular composition tetrahedron for four component system.

In the tetrahedron, a plane through the edge CD such as CDd has the useful property that any composition represented by a point in this plane has the same ratio n_A:n_B. From a point d′ on the line dC, a line d′D has the proportion d to C constant, and as d has A and B in constant proportion, a line d′D has n_A:n_B:n_C constant and, as for the ternary already described, as the composition moves upward along d′D, μD must increase, since:

$$\mu_D = \left(\frac{\partial G}{\partial n_D}\right)_{T,P,n_A,n_B,n_C} \qquad (12)$$

Similarly for a line from any point on dD to C, μ_C must increase as C is approached.

μ_D and μ_C can be plotted against one another for a given d. A third axis normal to the μ_D - μ_C plane can then give $X_B = n_B/(n_A + n_B)$, Figure 19.

The ternaries ACD and BCD are plotted on the two parallel vertical planes of Figure 19. Tie-lines are horizontal lines, parallel to the X_B axis. Tie-lines join surfaces which are the boundaries of single-phase regions. A section taken at constant μ_D, say, gives a μ_C versus X_B figure similar to that in a ternary system.

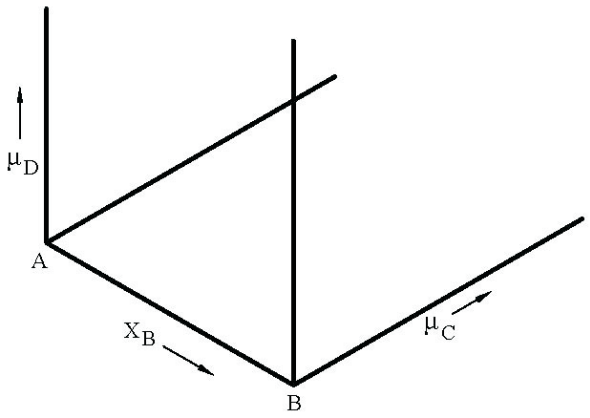

FIG 19 - Variation of μ_D and μ_C for the A-B-C-D four component system.

A tie-line projects as a point in the μ_D - μ_C planes. If μ_D is varied, the point traces out a line in this plane.

THE Cu-Fe-S-O-SiO_2 SYSTEM – YAZAWA'S DIAGRAM

This is in effect a four-component system, since it is saturated with SiO_2. The following uses the same axes with composition $X_{Fe} = n_{Fe}/(n_{Fe} + n_{Cu})$ where Yazawa uses matte grade in Figure 1. This is a monotonic function of X_{Fe} except for mattes containing oxygen.

For the SiO_2 saturated system, at very low P_{S_2}, the Cu-Fe-O-SiO_2 will be as shown schematically in Figure 20. If P_{S_2} is increased, provided the effect of dissolved sulfur is negligible, Figure 20 will remain unchanged. The three-phase equilibrium line, Cu(l), Fe(s) and slag projects as a line on the $\log P_{O_2} - \log P_{S_2}$ diagram. Yazawa shows this as a horizontal line which ends at his point r (Figure 1).

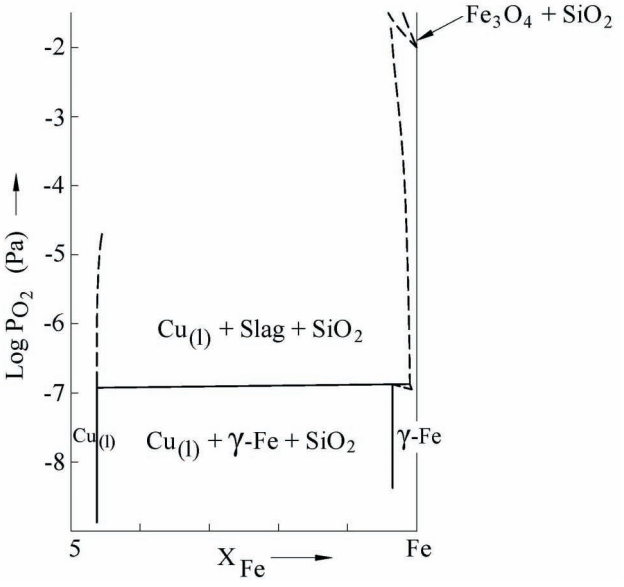

FIG 20 - The system Cu-Fe-O-$SiO_{2\ Sat}$.

Similar reasoning applies to the Cu-Fe-S matte, Figure 15. This is the base of Yazawa's figure (Figure 1). There is a three-phase line: Cu(l), matte, and Fe saturated system. This line

plots as a point on the $\log P_{O_2} - \log P_{S_2}$ plane. If P_{O_2} is increased without any appreciable effect on the equilibrium, the point traces a vertical line, and eventually meets the horizontal line at r. This vertical line is not shown on Yazawa's diagram.

At the point r two three-phase equilibria meet: Cu-Fe-matte and Cu-Fe-slag. Two new three-phase equilibria are now stable: Cu-matte-slag and Fe-matte-slag. These are shown by the lines rCs and rq respectively in Yazawa's diagram.

As P_{S_2} increases along rq, the matte becomes enriched in iron and at q, reaches the ternary Fe-S-O plane of the diagram with Fe, FeO-SiO_2 slag and $FeS_{(l)}$ in equilibrium at q. This matte contains oxygen and Yazawa puts $a_{FeS} = 0.66$ and for the slag $a_{FeO} = 0.3$, so for the line qp where:

$$FeS(l) + \tfrac{1}{2}O_2(g) = FeO \text{ (in } SiO_2 \text{ saturated slag)} + \tfrac{1}{2}S_2(g) \qquad (13)$$

P_{S_2} / P_{O_2} is fixed and the line qp has a slope of + 1.

It is assumed that the activity of FeS in the matte is determined *only* by the matte grade, independent of P_{S_2} or P_{O_2} then lines of constant matte grade have the same slope (45°), as Yazawa's diagram shows.

A section at P_{S_2} just higher than that at r is given schematically in Figure 21. When P_{S_2} is greater than that for the binary Cu(l)+Cu_2S, Cu is no longer a stable phase. Similarly, for P_{S_2} greater than that of q, Fe is no longer stable. At higher P_{S_2}, a vertical section shows only matte and slag equilibria. Figure 22 shows two such sections at different P_{S_2}. The section is similar to that already shown for three-component systems, because the variance is the same. The line a-a′ is a line of constant X_{Fe} (or Yazawa's constant matte grade). Yazawa's lines qp and rCs are the boundaries of the two-phase matte-slag equilibria. The steep slope of the latter is due to the rapid decrease in iron activity as matte becomes richer in Cu. The former small slope is due to the small change in activity of iron as P_{S_2} increases towards q.

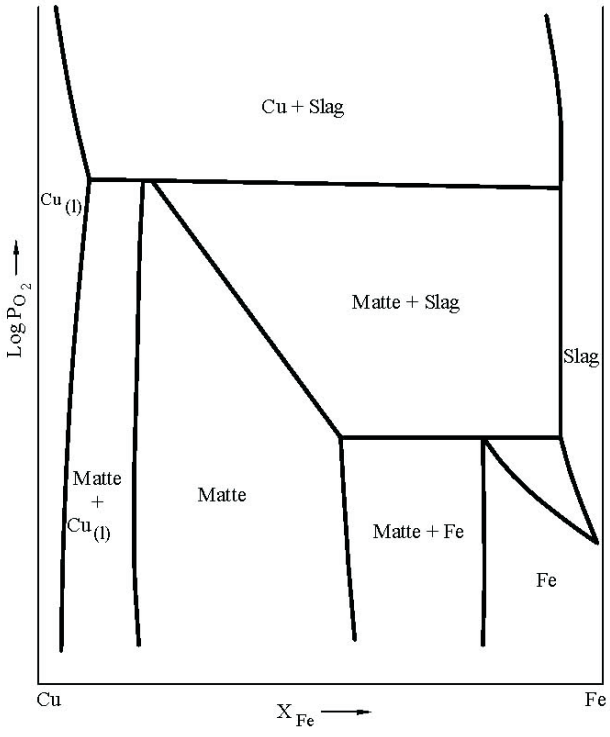

FIG 21 - Log P_{O_2} versus Cu-Fe in the Cu-Fe-O-S-SiO_2 Sat system. Section at slightly higher P_{S_2} than at r in Yazawa's diagram. Schematic log P_{S_2} constant.

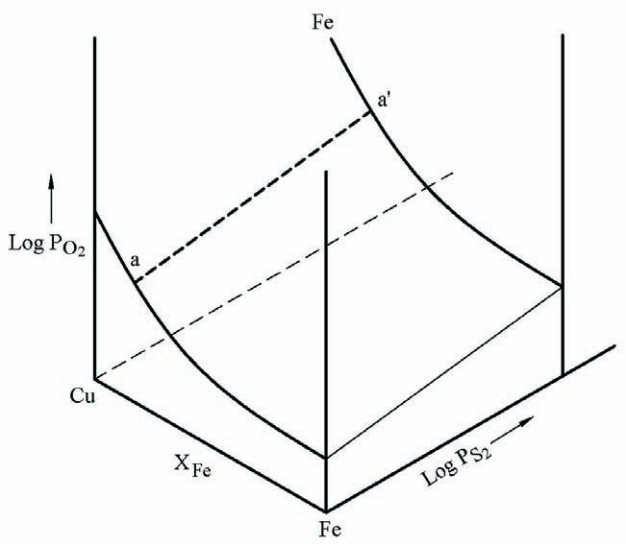

FIG 22 - Matte-slag surfaces.

With some hindsight, the essential matte-slag equilibria can be treated qualitatively as follows. For an isothermal condensed system, with four components Cu, Fe, S_2 and O_2, there are two degrees of freedom for the two phases. The tie-lines joining matte and slag are not shown. It is clear that slag copper content is not fixed by matte grade – there is still another degree of freedom.

Yazawa's diagram contains lines for constant P_{SO_2}. These are obtained from the equilibrium constant for the reaction $S_2(g) + 2O_2(g) = 2SO_2(g)$.

$$K = (P_{SO_2})^2 / (P_{S_2}) \cdot (P_{O_2})^2 \qquad (14)$$

from which:

$$P_{O_2} = \text{constant} - \tfrac{1}{2} \log P_{S_2} \qquad (15)$$

P_{SO_2} may be fixed by process conditions, and the course of oxidation followed along such an isobar.

Sections do not have to be taken at constant P_{S_2} (or P_{O_2}). Experimentally, for sulfide-oxide systems, constant P_{SO_2} is often convenient and P_{O_2} measurements can give a useful diagram. The Zn-Fe-S-O system was treated in this way by Espelund and Jynge (1977).

SYSTEMS WITH FIVE COMPONENTS

Yazawa's method of treating the Cu-Fe-S-O-SiO_2 as a four-component system by assuming saturation with SiO_2 throughout is one method of discarding a degree of freedom. Holding one activity constant can achieve the same result, eg constant P_{O_2} by the use of the gas mixture such as CO and CO_2.

COMPARISON WITH CONVENTIONAL DIAGRAM

The disadvantage of these diagrams as compared with conventional ones is that the composition is more or less ignored, or only given, for example, in terms of two components out of say four. This may be helped by labelling important points with the required composition. In the same way a conventional diagram may have some thermodynamic data added, eg log P_{O_2} in a metal-oxygen system. The two approaches are complementary.

ACKNOWLEDGEMENT

I am grateful to Dr John Floyd for his help and encouragement, to his colleagues at Ausmelt, and to Mr Jimmy Wong for his work on the diagrams.

REFERENCES

Aukrust, E A and Muan, A, 1963. Activities of components in oxide solid solutions: The systems CoO-MgO, CoO-MnO and CoO-'FeO' at 1200°C, *Trans Metall Soc AIME*, 227:1378-1380.

Baker, E H, 1974. *Trans Inst Min Met*, 83(817):C237-C240.

Bale, C W and Toguri, J M, 1976. Thermodynamics of the copper-sulfur, iron-sulfur and copper-iron-sulfur systems, *Can Metall Quart*, 14:1.

Chakraborti, N and Lynch, D C, 1983. Thermodynamics of roasting arsenopyrite, *Metall Trans*, 14B:239-251.

Chang, Y A, Neumann, J P and Choudary, U V, 1979. *Phase Diagrams and Thermodynamic Properties of Ternary Copper-Sulfur-Metal Systems* (The International Copper Research Association, INCRA: New York).

Ellingham, H J T, 1944. Reducibility of oxides and sulfides in metallurgical processes, *J Soc Chem Ind*, 63:125-133.

Erik, R H and Ozok, H, 1994. High-temperature phase relations and thermodynamics in the iron-lead sulfur system, *Metall and Mater Trans B*, 25B(1):53-61.

Espelund, A W and Jynge, H J, 1977. System Zn-Fe-S-O. Equilibria between sphalerite or wurtzite, pyrrhotite, spinel, ZnO and a gas phase, *Scand J Metall*, 6:256-261.

Hino, M and Toguri, J M, Personal communication.

Ingraham, T R, 1964. Thermochemistry of the Co-S-O system from 950 to 1200°K, *Can Metall Quart*, 3:221-234.

Ingraham, T R, 1965. Thermodynamics of the thermal decomposition of cupric sulfate and cupric oxysulfate, *Trans Met Soc AIME*, 233:359-363.

Ingraham, T R, 1966. Thermodynamics of the Mn-S-O system between 1000°K and 1250°K, *Can Metall Quart*, 5:109-122.

Ingraham, T R and Kellogg, H H, 1963. Thermodynamic properties of zinc sulfate, zinc basic sulfate, and the system Zn-S-O, *Trans Metall Soc AIME*, 227:1419-1426.

Jacob, K T, Fitzner, K and Alcock, C B, 1977. Activities in the spinel solid solution, phase equilibria and thermodynamic properties of ternary phases in the system Cu-Fe-O, *Metall and Mater Trans B*, 8(2):451-460.

Kellogg, H H and Basu, S K, 1960. Thermodynamic properties of the system lead-sulfur-oxygen to 1100°K, *Trans Metall Soc AIME*, 218:70-81.

Korzhinskii, D S, 1959. *Physiochemical Basis of the Analysis of the Paragenesis of Minerals* (Consultant Bureau: New York).

Lin, J-C, Sharma, R C and Chang, Y A, 1986. The Pb-S (lead-sulfur) system, *Bulletin of Alloy Phase Diagrams*, 7(4):374.

Pelton, A D and Schmalzried, H, 1973. On the geometrical representation of phase equilibria, *Metall Trans*, 4(5):1395-1404.

Schmalzried, H and Pelton, A D, 1973. Zur geometrischen Darstellung von Phasengleichgewichten, *Berichte der Bunsengesellschaft für Physikalische Chemie*, 77:90-94.

Schmid, R, 1983. A thermodynamic analysis of the Cu-O system with an associated solution model, *Metall and Mater Trans B*, 14(3):473-481.

Sharma, R C and Chang, Y A, 1979. Thermodynamics and phase relationships of transition metal-sulfur systems: Part III. Thermodynamic properties of the Fe-S liquid phase and the calculation of the Fe-S phase diagram, *Metall and Mater Trans B*, 10(1):103-108.

Sharma, R C and Chang, Y A, 1980. Thermodynamics and phase relationships of transition metal-sulfur systems: IV. thermodynamic properties of the Ni-S liquid phase and the calculation of the Ni-S phase diagram, *Metall and Mater Trans B*, 11(1):575-583.

Skeaff, J M, Mainwaring, P R and Speelman, J L, 1985. Thermochemical arsenide-oxide equilibria in the system nickel-arsenic-oxygen determined electrochemically between 438 and 866°C, *Can Metall Quart*, 24:349-362.

Willis, G M, unpublished.

Yazawa, A, 1974. Thermodynamic considerations of copper smelting, *Can Metall Quart*, 13(3):443-455.